Available online at www.sciencedirect.com
SCIENCE DIRECT
Journal of Hydrology 326 (2006) 43–58
Journal of Hydrology
www.elsevier.com/locate/jhydrol

Numerical experiments on the sensitivity of runoff generation to the spatial variation of soil hydraulic properties

Michael Herbst [a,*], Bernd Diekkrüger [b], Jan Vanderborght [a]

[a] Agrosphere Institute, ICG-IV, Forschungszentrum Jülich GmbH, D-52425 Jülich, Germany
[b] Hydrology Research Group, Department of Geography, University Bonn, Meckenheimer Allee 166, D-53115 Bonn, Germany

Received 3 May 2005; revised 18 October 2005; accepted 20 October 2005

Abstract

Spatially distributed soil hydraulic properties are required for distributed hydrological modelling. These soil hydraulic properties are known to vary significantly in space, and considering the non-linearity of runoff generation, the question arises how the spatial variation of soil hydraulic parameters affects the continuous runoff modelling for a micro-scale catchment. This was analysed by applying a three-dimensional hydrological model to the 28.6 ha 'Berrensiefen' catchment, Germany, for a simulation period of one year. The model was based on an observed distribution of soil hydraulic properties, which were assumed to be layered in vertical and to vary continuously in horizontal direction, and validated for total runoff. Numerical experiments with five spatial distributions of soil hydraulic parameters derived from the observed spatial distribution, which was supposed to be the 'true' underlying spatial variation, were carried out. These five spatial concepts were: choropleth map, spatially homogeneous case, random distribution, stochastic simulation and conditional stochastic simulation. The comparative modelling revealed a significant sensitivity of runoff generation towards the spatial variation of soil hydraulic properties. The comparison of the hydrograph of surface and macropore runoff to the initial model runs exhibited the highest root mean square error with 1.3 mm h^{-1} for the homogeneous case. Further we detected, that the frequency distribution of soil hydraulic properties played an important role for the reproduction of runoff amounts. But also the spatial topology (deterministic spatial variation) was relevant for an adequate description of runoff generation. Conditional stochastic simulation is seen as a promising approach, because it preserved both, the frequency distribution and the deterministic variation.

Keywords: Conditional stochasic simulation; Soil mapping; Macropore runoff; Soil hydraulic properties; Spatial variation; Soil heterogeneity

1. Introduction

The spatial arrangement of soils, topography, geology and land cover determines the spatial pattern of hydrological processes (Grayson and Blöschl, 2001). The spatial data used for hydrological modelling are often treated as variables with discreet spatial units of averaged parameter values (Zhu and

* Corresponding author. Tel.: +49 2461 618674; fax: +49 2461 612518.
E-mail addresses: m.herbst@fz-juelich.de (M. Herbst), b.diekkrueger@uni-bonn.de (B. Diekkrüger), j.vanderborght@fz-juelich.de (J. Vanderborght).

0022-1694/$ - see front matter © 2005 Elsevier B.V. All rights reserved.
doi:10.1016/j.jhydrol.2005.10.036

Mackay, 2001). Such kind of a spatial concept might be suitable for several variables, like e.g. a classified land cover. Nevertheless, the question arises, whether such a spatial concept is appropriate for the spatial pattern of soil properties (Burrough, 1993; Webster, 2000; Heuvelink and Webster, 2001) and in particular for soil hydraulic parameters. These are known to vary significantly in space (Warrick and Nielsen, 1980; Vereecken et al., 1997) and to strongly affect hydrologic processes such as runoff generation. Soil parameters show a distinct layering in the vertical direction, allowing for a spatial concept of discrete boundaries. But soil properties are assumed to vary continuously in the horizontal direction. The question arising now is: How does the spatial aggregation of soil hydraulic properties in horizontal direction affect the hydrological response? This is particularly relevant against the background of the non-linear relation between soil parameters and water fluxes (Beven, 2001). Here the upper part of the unsaturated zone plays an important role for the runoff process by splitting up the precipitation into two fractions: infiltration and infiltration excess, which becomes surface runoff (Hortonian overland flow) or macropore runoff.

The significant influence of the spatial variability of soil moisture as an initial condition for an event based modelling of runoff was already investigated in detail (Merz and Plate, 1997; Bronstert and Bardossy, 1999; Zehe and Blöschl, 2004). Seyfried and Wilcox (1995) distinguished between deterministic and stochastic spatial variability and pointed out that often geostatistical methods were applied capturing the stochastic variability but neglecting the deterministic variability. This distinction between stochastic and deterministic variability was taken up by Merz and Bardossy (1998). They used an event-based model to determine the effect of the spatial variability of the water content at saturation and the saturated hydraulic conductivity on runoff and detected, that a structured (deterministic) variability created larger runoff amounts than a purely stochastic variability. Loague (1988); Loague and Corwin (1996) used a Monte-Carlo approach for the spatial variability of the saturated hydraulic conductivity of a synthetic hillslope and proved a high relevance of this parameter for the description of infiltration processes. Loague and Kyriadikis (1997) applied stochastic simulations (Sequential Gaussian Simulation) for a small catchment to capture the spatial variation of saturated hydraulic conductivity. This approach led to a slightly improved runoff prediction compared to simulations using saturated hydraulic conductivities obtained by simple averaging or by kriging.

Due to the computational effort three-dimensional water flow modelling applications for catchments are still rather sparse. The first layout for a three-dimensional model of unsaturated water fluxes was developed by Freeze (1971). First three-dimensional catchment modelling was enabled by codes like SHE (Abbott et al., 1986) or IHDM (Beven et al., 1987). Binley et al. (1989a) developed a three-dimensional finite element model and applied it in a first step to a synthetic hillslope (100×150 m) with a spatially variable hydraulic conductivity. In the second step Binley and Beven (1992) applied this model for a 25 ha catchment with a homogeneous saturated hydraulic conductivity in horizontal direction. This model system was further developed by Paniconi and Wood (1993) and was applied to a micro-scale catchment of 24 ha size with a 30 m grid in horizontal direction. A more recent development is the event-based HILLFLOW3d (Bronstert and Plate, 1997), which was used to model the variably saturated water fluxes under consideration of macropores for a 33 ha catchment. To demonstrate the uncertainty in initial soil water contents for event-based runoff simulations, Loague et al. (2005) applied the 3d Integrated Hydrology Model (InHM; VanderKwaak and Loague, 2001) to the 10 ha R-5 catchment. An overview of selected physically-based models related to near-surface hydrologic-response processes is given by Loague and VanderKwaak (2004).

In this study SWMS_3d (Šimůnek and Huang, 1995) was extended by a macropore runoff submodel. A runoff delay routine was applied to continuously model the hydrological processes of a 28.6 ha catchment for one year. This model, using a continuous spatial structure for the hydraulic properties of two soil horizons, was validated against measured runoff. The spatial structures of soil hydraulic properties were derived from a point data set on soil textural properties in combination with a pedo-transfer function and in dependence of terrain attributes using regression kriging (Herbst et al., 2006). Using this observed spatial structure as the

'true' underlying structure allows the test of several spatial concepts including stochastic and deterministic approaches as well as a mixture of both. This study has two main objectives: (i) to quantify the sensitivity of runoff generation concerning the spatial distribution of soil physical properties for a continuous hydrological process model, and (ii) to determine the most appropriate concept of soil spatial variation for the modelling of catchment scale runoff processes.

2. Methods and data

2.1. Test area

The 'Berrensiefen' catchment (28.6 ha) is located 25 km north–east of Bonn, Germany (long. 07°27′E, lat. 50°55′N), at an altitude of 231–303 m a.s.l. It is a small rural sub-catchment of the river Rhine. A relative high mean value of precipitation was measured with 1046 mm a^{-1}(long term mean, measured at the nearby 'Wahnbach' reservoir), leading to significant amounts of runoff. Due to the rather thin soil layer and the low conductive underlying bedrock the fast runoff components, surface runoff and macropore runoff, dominate the runoff generation.

The soils were mainly derived from solifluidal layers of the underlying bedrock of the devonian period. A north/north–west directed fault divides the catchment into two parts of almost similar size. The western part is dominated by silt stone and the eastern part is mainly sand stone. The overall depth of the predominating Haplic Luvisol (FAO et al., 1998) ranged from roughly 0.5 m at the ridge to 1.3 m at the lower parts of the slope. Stagnic Luvisols are found at concave shaped locations due to lateral hypodermic flow, whereas Eutric Gleysols are found close to the channel network. Large fractions of rock fragments close to the soil surface are common on ridge and upslope areas. In the valley floor nearly rock free profiles are found. Soil texture ranged from sandy to silty loam. In general, the landscape is gently sloping (Fig. 1) with an average slope of 10.9° and a westerly aspect. Only the upper parts of the channel showed deep valley cuts with slopes up to 14°. Pasture clearly predominate the catchment, covering an area of about 82%. Only the upper north-eastern part is forested.

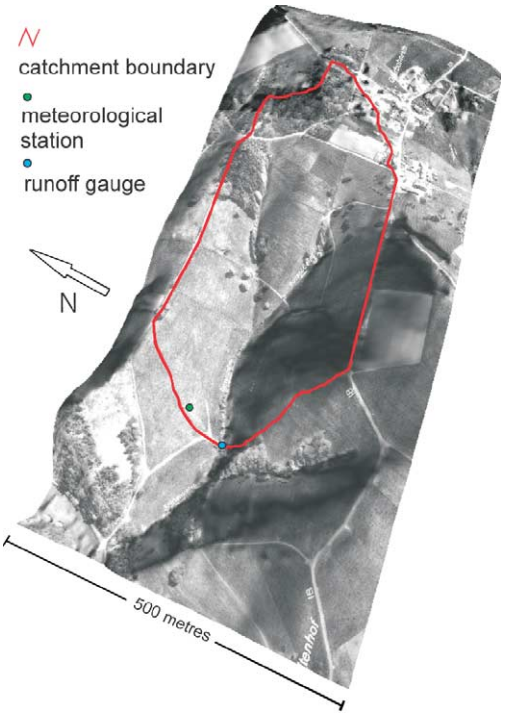

Fig. 1. Aerial view of the 'Berrensiefen' catchment.

2.2. Hydrological process model

The spatio-temporal variation of hydrological processes was simulated with a modified version of SWMS_3d (Šimůnek and Huang, 1995), which was coupled to a module describing the atmospheric boundary conditions. This module calculated snowmelt with the degree-day method, canopy interception with a bucket model (Rutter et al., 1975) and the potential evapotranspiration for forest and pasture according to the Penman/Monteith approach (Monteith, 1975) from measured meteorological parameters. SWMS_3d was used to model soil water movement, infiltration excess, drainage, root water uptake (Feddes et al., 1978) and actual evaporation. The three-dimensional variably saturated water flow was given by:

$$\frac{\partial\theta(\mathbf{s},t,h)}{\partial t} = \nabla(\mathbf{K}(\mathbf{s},h)\nabla H(\mathbf{s},h)) + Q(\mathbf{s},t) \quad (1)$$

where θ is the volumetric water content (L^3L^{-3}), **K** is the hydraulic conductivity tensor (LT^{-1}), **s** is the

position vector in a three-dimensional space, h is the pressure head (L), H is the total head (L), Q is the source/sink term (T^{-1}) and t is time (T). This mixed form equation (Eq. 1) was solved in a numerical scheme using finite elements for the spatial discretization and Picard iteration with finite differences for the temporal discretization. The amount of surface runoff was calculated from the infiltration excess estimated with the Richards equation (Eq. 1). Modifications of the original SWMS_3d code include a simplified approach for the interaction between macropore and matrix infiltration:

$$Q_{\mathrm{sur}} = \begin{cases} 0 & I_e \le \mathrm{I}_{mac} \\ I_e - \mathrm{I}_{mac} & I_e > \mathrm{I}_{mac} \end{cases} \quad \text{and} \quad Q_{\mathrm{mac}} = \begin{cases} I_e & I_e \le \mathrm{I}_{mac} \\ \mathrm{I}_{mac} & I_e > \mathrm{I}_{mac} \end{cases} \tag{2}$$

where Q_{sur} is the surface runoff (L T^{-1}), I_e is the matrix infiltration excess (L T^{-1}), I_{mac} is the maximum macropore infiltration (L T^{-1}) and Q_{mac} is the macropore runoff (L T^{-1}). Surface runoff occurred if the matrix infiltration excess was larger than the macropore infiltration capacity. It was assumed that macropore flow entered the channel as interflow without interaction with the soil matrix. For matrix infiltration a flux boundary (Neumann) was applied to the uppermost node until a given pressure head (-0.001 cm) was reached. At this point SWMS_3d fixed this pressure head and switched to the Dirichlet boundary condition, thus infiltration decreases and converges to a value close to the saturated hydraulic conductivity. Further extensions included a two-dimensional runoff module. Macropore and surface runoff were delayed by a travel time,

$$t_q = \Omega_s \cdot F_l \tag{3}$$

where t_q is the travel time (T), Ω_s is the system resistance (T L^{-1}) and F_l is the length of the flow path to the channel (L), which was calculated from the 5-m digital elevation model. For this flow routing the Multiple Flow Direction Algorithm of Freeman (1991) was adopted. By reaching the channel the runoff was supposed to appear immediately at the catchment outlet, because the travel time of the runoff in the channel (length of the channel $\sim$450 m with a flow velocity in the channel of $\sim$0.5 m s^{-1}) was clearly shorter than the process model time step of 1 h. The runoff module allows the estimation of the time between runoff generation at a certain location and the runoff reaching the channel. For the surface runoff, the system resistance Ω_s can be understood as a roughness parameter. In the channel no routing was applied. For the groundwater runoff the amount of drainage estimated at the bottom of the soil profile (see also next Section 2.3) was supposed to appear instantaneously at the catchment outlet. This assumption only holds for catchments with very little groundwater retention, like the one selected for this study.

2.3. Model set up

2.3.1. Model domain

At the top of the model domain the atmospheric boundary condition was applied. Maximum Infiltration rate of the macropores and system resistances were determined by a stepwise calibration procedure. Maximum infiltration rate into the macropore system was set to 7.0 mm h^{-1}. The system resistances were set to 6.6×10^{-4} s $m^{-1}$and 2.9×10^{-5} s m^{-1} for the macropore and the surface runoff, respectively. At the bottom boundary a seepage face condition was imposed and groundwater runoff was simply set equal to the drainage amount. The groundwater runoff was supposed to appear instantaneous at the catchment outlet, without any routing. A no-flow boundary condition was imposed at the lateral domain boundaries. The digital elevation model was used to reconstruct surface morphology. The spatial discretization of the model was given by a 10 m quadratic grid in horizontal direction and five nodes in vertical direction with a variable spacing depending on soil thickness. The mesh consisted of 21856 nodes. Topsoil thickness was interpolated using a kriging of areal residuals from point measurements in dependence of the land use, varying between 5.6 cm in the forested part up to 20.2 cm for the agricultural soils (Fig. 2). The subsoil thickness was interpolated by regression kriging from point measurements and terrain attributes. Mean subsoil thickness is 68.7 cm. Details on the interpolation procedures for both horizons can be found at Herbst et al. (2006). The soil thickness was kept constant for all model runs.

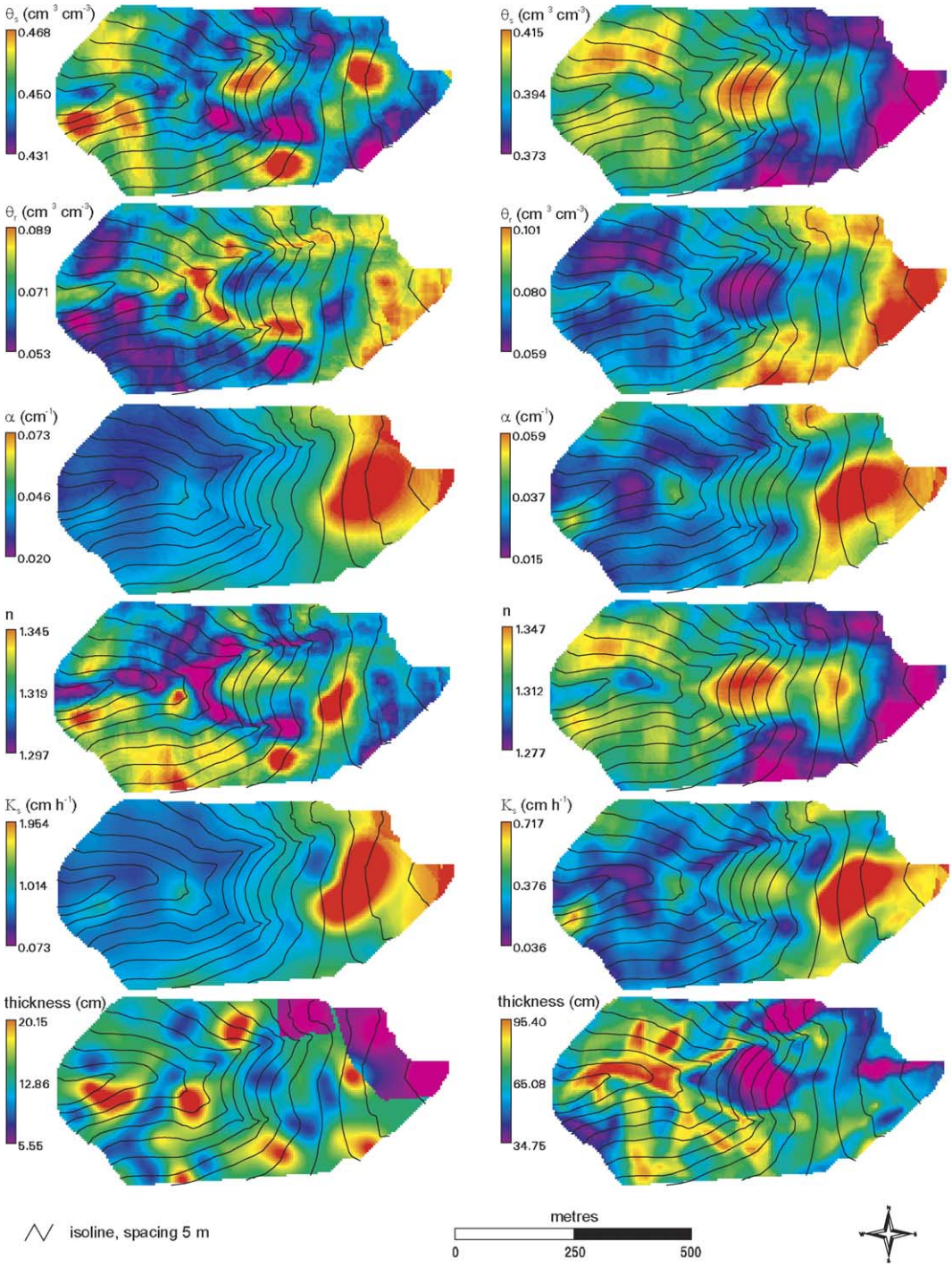

Fig. 2. Observed spatial patterns of the Mualem/van Genuchten parameters and soil thickness for the topsoil (left) and the subsoil (right).

2.3.2. Observed distribution of soil hydraulic properties

The observed distribution of soil hydraulic properties was based on the parameters according to Mualem/van Genuchten (van Genuchten, 1980). The following five parameters were required: θ_r is the residual water content ($cm^3\,cm^{-3}$), θ_s is the water content at saturation ($cm^3\,cm^{-3}$), α is the inverse of the bubbling pressure (cm^{-1}), n (−) is a dimensionless shape parameter, and K_s ($cm\,h^{-1}$) is the saturated hydraulic conductivity. In order to derive these parameters 65 samples were taken for the topsoil and 47 samples were taken for the subsoil. Those samples were analysed for particle size distribution and the pedotransfer-functions (PTF) of Rawls and Brakensiek (1985) were applied to this point data set. The PTF of Brakensiek and Rawls (1994) was also applied to modify θ_r, θ_s and K_s in dependency of the coarse fraction (>2 mm). In order to estimate the spatial pattern of the Mualem/van Genuchten parameters a combined method of kriging and regression (Odeh et al., 1995) with terrain attributes was used. Further details about the generation of this observed distribution are given by Herbst et al. (2006). Fig. 2 shows the spatial distributions of the soil hydraulic parameters. A good example for the spatial correlation between a soil hydraulic parameter and topography is topsoil θ_r. High values of the residual water content were found rather close to the channel network, whereas small values were typically located at convex surface shapes and on uplsope areas close to the watershed. This was mainly a result of high clay contents detected close to the channel network, which yields high residual water contents. Fig. 2 also reveals the auto-correlation of the Mualem/van Genuchten parameters (Vereecken and Herbst, 2005), which is preserved by the PTF. For example θ_s is negatively correlated with θ_r as well as the spatial pattern of α is positively correlated with K_s. The spatial distribution of the topsoil hydraulic parameter is basically resembled by the respective subsoil parameter. Table 1 summarizes main statistical features of the observed distribution. The parameter ranges were typical for silty and sandy loam. In general, the variances were rather moderate, which was mainly the result of the relative homogeneous spatial distribution of the textural composition. However, topsoil and subsoil K_s revealed a significant variability covering almost one order of magnitude. The K_s-values initially calculated with the PTF were scaled down by 0.5 during model calibration. This was necessary because K_s of the soil matrix measured in this catchment (Bogena et al., 2003) was on average lower than predicted by the PTF. The number of this K_s measurements was too small to be used for the estimation of the spatial structure of K_s. Layered soils often exhibit a higher saturated hydraulic conductivity in the horizontal direction (Hodgkinson and Armstrong, 1996). Thus, the global anisotropy of the saturated hydraulic conductivity was assumed to be one magnitude higher in horizontal direction, which was also relevant to describe the downslope soil water movement (Herbst

Table 1
Descriptive statistics of the residual water content θ_r, the saturated water content θ_s, the inverse of the bubbling pressure α, the shape parameter n, and the saturated hydraulic conductivity K_s for the topsoil and the subsoil of the observed distribution

	Mean	Standard deviation	Min	Max
Topsoil				
θ_r ($cm^3\,cm^{-3}$)	0.075	0.005	0.053	0.089
θ_s ($cm^3\,cm^{-3}$)	0.446	0.005	0.431	0.468
$Log_{10}(\alpha\ (cm^{-1}))$	−1.480	0.133	−1.707	−1.134
n (−)	1.319	0.007	1.297	1.345
Log_{10} (K_s ($cm\,h^{-1}$))	−0.488	0.284	−1.139	0.291
Subsoil				
θ_r ($cm^3\,cm^{-3}$)	0.077	0.009	0.059	0.101
θ_s ($cm^3\,cm^{-3}$)	0.396	0.009	0.373	0.415
Log_{10} (α (cm^{-1}))	−1.543	0.121	−1.813	−1.226
N (−)	1.316	0.015	1.277	1.347
Log_{10} (K_s ($cm\,h^{-1}$))	−0.721	0.228	−1.445	−0.145

and Diekkrüger, 2003). Due to the spacing of sampling locations and the use of a 10-m grid in horizontal direction for the modeling any small scale variation of soil hydraulic properties was smoothed out and parameter values were treated as effective hydraulic parameters relevant to this spatial scale.

2.3.3. Concepts of soil spatial variation

The observed distribution described above was used to generate five spatial distributions of soil hydraulic parameters: choropleth map, homogeneous, random, stochastic simulation and conditional stochastic simulation.

Commonly applied soil maps are based on the concept of choropleth maps. Basic assumption of this classification approach is that the within-class variance is smaller than the overall variance. The spatial variability of the value z_{ij} of a soil property Z at location x_i in soil class j was defined as:

$$z_{ij} = \mu + \alpha_j + \varepsilon_{ij} \tag{4}$$

where μ is the total mean of Z, α_j is the difference between μ and the mean of soil class j, and ε_{ij} is a random component with zero mean. The estimated value z^*_{0j} for the location x_0 is the arithmetic mean of the n_j sample values z_{ij} in the class j,

$$z^*_{oj} = \frac{1}{n_j}\sum_{i=1}^{n_j} z_{ij} \tag{5}$$

To generate a choropleth map according to this approach the polygons of the available 1:5000 soil map were used. The grid values of the observed distributions were taken as sample points of soil hydraulic properties for the soil units. Thus, we applied the geometry of the common soil map, but we assigned the respective mean values of the observed distribution to the single polygons. For the Mualem/van Genuchten parameters α and K_s a significant skewness was detected, thus both of these parameters were transformed with the decadic logarithm prior to the averaging. For the *homogeneous* spatial concept the parameters were handled similarly to the choropleth approach with the difference, that the whole catchment area was treated as one single polygon with one Mualem/van Genuchten parameter set for the topsoil and one for the subsoil. Thus, spatial variability was neglected.

For the random spatial concept, the parameters for the topsoil and the subsoil were randomly distributed across the grid cells. In this way, the frequency distribution of the observed distribution was preserved, but the spatial structure was lost, a texture was generated.

For the stochastic simulation the pattern is random too, but the spatial auto-correlation was considered. This approach is based on the theory of the regionalized variable (Matheron, 1973). For the quantification of the spatial auto-correlation the experimental semi-variance γ_e was determined,

$$\gamma_e(l) = \frac{1}{2n(l)}\sum^{n(l)} (Z(x_i) - Z(x_j))^2 \tag{6}$$

where l (m) is the distance between two sampling points x_i and x_j of the variable Z, and n is the number of observations. The distance l was classified because the number of sample pairs is finite. Since the semi-variance for any given distance was required, a theoretical variogram was fitted to the experimental semi-variance. Several variance models are available (Wackernagel, 1995), for this study only gaussian semi-variances γ_g without a nugget effect were used:

$$\gamma_g(l) = \begin{cases} c_1[1 - e^{(l^2/a^2)}] & \text{for } l \le a \\ c_1 & \text{for } l > a \end{cases} \tag{7}$$

where c_1 is the sill, l is the lag distance (m) and a is the range (m). Using a stochastic simulation, random and equally probable models of spatial distribution could be generated based on the mean and the spatial auto-correlation function of the variable. For this we adopted the turning bands method (TBM; Mantoglou and Wilson, 1982) in this study. The semi-variograms were fitted with the VESPER-software (Minasny et al., 1999).

The equally probable parameter fields that are obtained using stochastic simulation are independent and not correlated with the parameter values measured or derived at the sampling points, i.e. unconditional parameter fields. In a conditional stochastic simulation, parameter fields are generated, which are perfectly correlated with the measured parameter values, i.e. at the sampling locations simulated and measured parameters are identical.

The conditionally estimated parameter at location x, $Z_c(x)$ was estimated as (Deutsch and Journel, 1998):

$$Z_c(x) = Z^*(x) + (Z_{uc}(x) - Z^*_{uc}(x)) \quad (8)$$

where $Z_{uc}(x)$ is the parameter value at location x in an unconditional realisation of the parameter field, $Z^*(x)$ is the kriged parameter based on the measurements and $Z^*_{uc}(x)$ is the kriged parameter based on the parameter values at the measurement locations in the unconditional realisation of the parameter field. The kriged parameter is derived from the parameter values at the measurement locations x_i as:

$$Z^*(x) = \sum_i^n \lambda_i Z(x_i) \qquad \text{with} \quad \sum_{i=1}^n \lambda_i = 1 \quad (9)$$

where n is the number of sample locations and λ_i are the kriging weights. The original sample locations (Fig. 5), 65 and 47 points for topsoil and subsoil respectively, were used to condition the stochastic simulation by ordinary block kriging.

3. Results

3.1. Hydrological process model validation

The simulation period started on September, 1st 1998 and ended one year later on August, 31th 1999. The model was calibrated for the first 2448 h (until December 11th 1998). The system resistances and the macropore infiltration capacity were calibrated against the measured runoff. In general, the simulated runoff was in good agreement with the observations (Fig. 3). This was also proven with a Coefficient of Model Efficiency ($-\infty < \text{CME} < 1$; Nash and Sutcliffe, 1970) of 0.56, an Index of Agreement ($0 < \text{IA} < 1$; Willmott, 1981) of 0.90 and a correlation coefficient of 0.83. Fig. 3 shows a measured hydrograph highly variable in time. It is also shown that the peak runoff of the several storm events was well captured by the model. Difficulties for the runoff simulation occurred during winter (~timestep 2550). This was mainly the result of a snowmelt event, which was not adequately captured by the degree-day method. Fig. 3 also shows that during summer (~after timestep 6000) the discharge decreases dramatically, indicating that groundwater runoff provided usually only a small fraction to the total discharge. During the simulation period a clearly above average amount of 1600 mm of precipitation were measured, of which 1220 mm became runoff. The simulated amount of total runoff was 1184 mm, whereas the estimated actual evapotranspiration for the catchment was 575 mm.

3.2. Sensitivity of runoff generation

The geostatistical spatial concepts considered during this study require the calculation of experimental semi-variograms and the fitting of theoretical semi-variograms in determining sill and range. This was necessary because for the generation of the observed distribution only semi-variograms of the variable residues were used. For the computation of the experimental semi-variograms the whole grid was sampled for every soil hydraulic parameter.

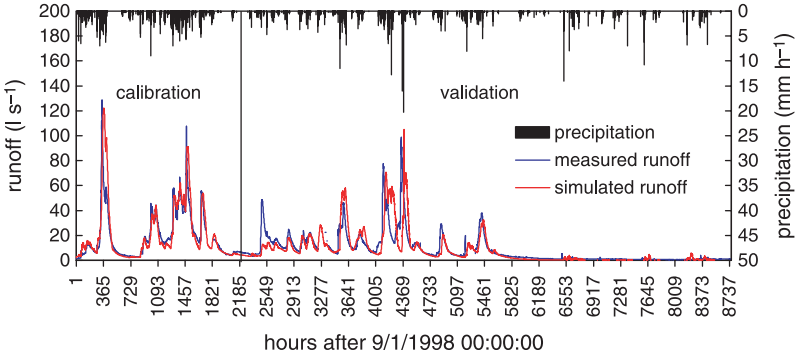

Fig. 3. Precipitation (mm h^{-1}), measured and simulated runoff (l s^{-1}) for the 'Berrensiefen' catchment.

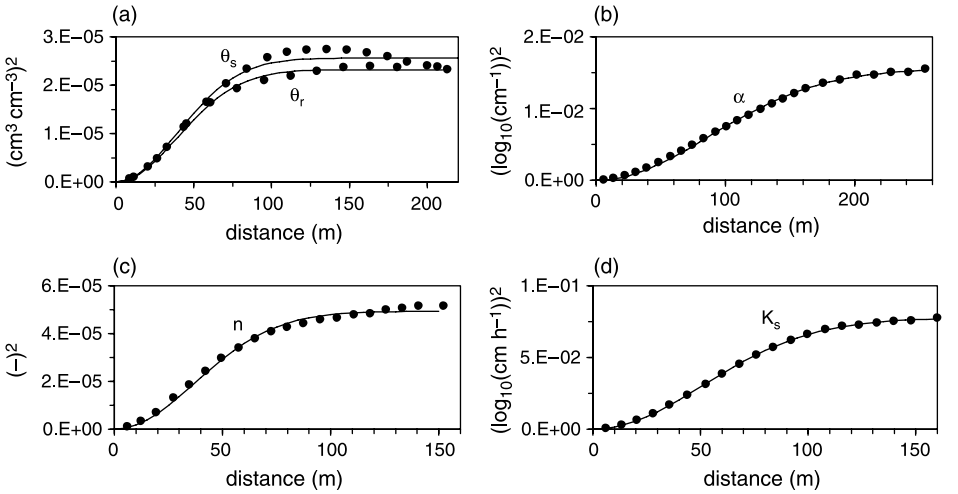

Fig. 4. Experimental (dots) and fitted theoretical semi-variograms (lines) of the topsoil observed distribution for the residual water content and the water content at saturation (a), the inverse of the bubbling pressure (b), the shape parameter (c) and the saturated hydraulic conductivity (d). The geostatistical parameters are given in Table 2.

As an example Fig. 4 shows the experimental and the fitted theoretical semi-variograms for the topsoil. It is clearly visible, that the fitted semi-variograms are in good agreement to the experimental semi-variograms. Thus an accurate estimation of range and sill was possible, with the slight exception of the Mualem/van Genuchten parameter θ_s. For this parameter the experimental semi-variogram revealed a weak 'hole effect': After reaching a sill the semi-variance decreases at a distance of roughly 150 m and increases again for larger distances. This 'hole effect' is often found for variables that vary periodically in space (Armstrong, 1998). This can probably be explained by the fact that in catchments the simplified pattern slope/drainage line/slope exists. Increasing the distance between sample points may decrease semi-variance because upslope positions on opposite slopes may be more similar than upslope-downslope positions. This 'hole effect' was found for topsoil θ_s and subsoil parameter n. Table 2 summarizes the geostatistical parameters of the soil hydraulic parameters for topsoil and subsoil. The ranges vary between 56 and 123 m. Concerning the spatial variability, the sills basically show the same picture as indicated by the standard deviations (Table 1). A high variability was found for topsoil and subsoil K_s. Table 2 also reveals that within a soil horizon θ_s and θ_r show almost similar sills and ranges. For the spatial aggregation approaches (homogeneous case and choropleth map) prior to the averaging the soil hydraulic parameters α and K_s were $\log_{10}$-transformed due to their skewed frequency distribution and re-transformed after the averaging. As an example Fig. 5 shows the spatial concept realizations for topsoil K_s. The observed distribution showed relative large saturated hydraulic conductivities in the upper eastern part of the catchment. Rather small K_s-values were found in the western part, particularly close to the channel

Table 2
Geostatistical parameters of the fitted theoretical semi-variograms for the residual water content θ_r, the saturated water content θ_s, the inverse of the bubbling pressure α, the shape parameter n, and the saturated hydraulic conductivity K_s

	Sill c_1	Range a (m)
Topsoil		
θ_r ($cm^3\ cm^{-3}$)	2.32×10^{-5}	55.6
θ_s ($cm^3\ cm^{-3}$)	2.56×10^{-5}	56.5
$\log_{10}(\alpha\ (cm^{-1}))$	1.55×10^{-2}	123.4
n (−)	4.93×10^{-5}	52.7
$\log_{10}$ (K_s ($cm\ h^{-1}$))	7.74×10^{-2}	72.7
Subsoil		
θ_r ($cm^3\ cm^{-3}$)	6.36×10^{-5}	102.0
θ_s ($cm^3\ cm^{-3}$)	6.42×10^{-5}	98.6
$\log_{10}$ (α (cm^{-1}))	1.86×10^{-2}	67.5
n (−)	2.04×10^{-4}	85.3
$\log_{10}(K_s$ ($cm\ h^{-1}$))	8.84×10^{-2}	58.1

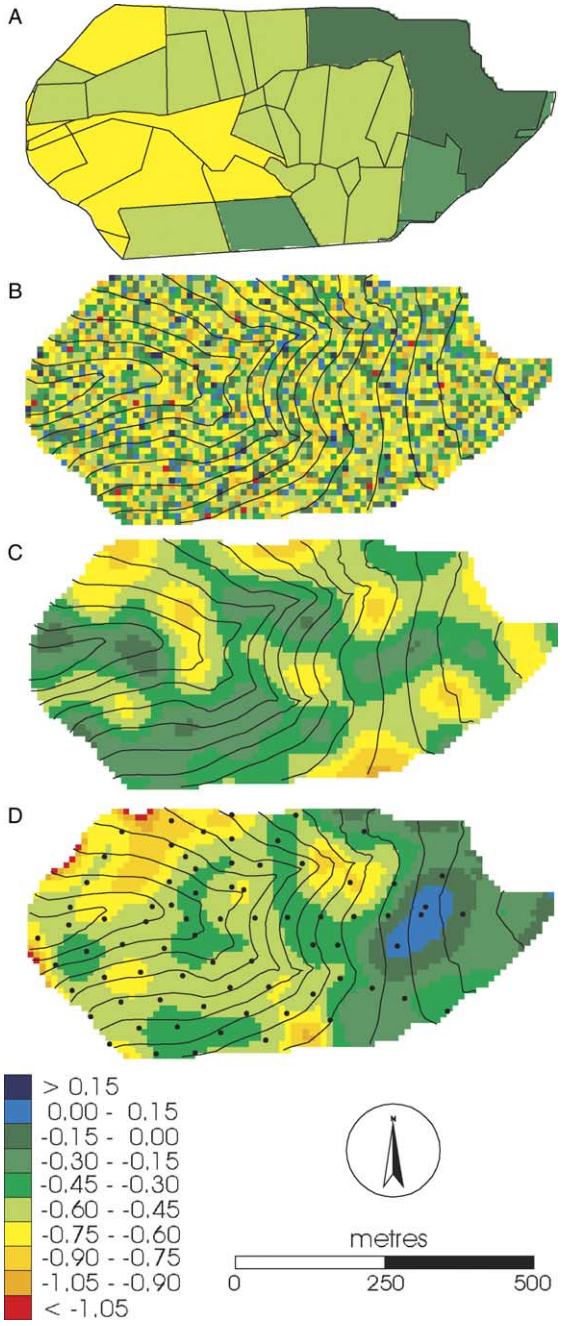

Fig. 5. Log_{10} of the topsoil saturated hydraulic conductivity for the spatial concepts: (A) choropleth map, (B) random, (C) stochastic simulation, and (D) conditional stochastic simulation. Sub-Fig. (D) also shows the location of the topsoil sample points. Isoline spacing is 5 m.

network. This spatial topology was basically resembled in the choropleth map (Fig. 5(A)), although obviously the extreme values of the frequency distribution were lost due to the averaging. The topology was basically resembled by the conditional stochastic simulation also (Fig. 5(D)), but the frequency distribution was preserved better than by the choropleth map. Fig. 5(C) shows that a non-conditional stochastic simulation preserved the spatial auto-correlation, but the topology was completely lost. This is also true for the random case (Fig. 5(B)). For this spatial concept the frequency distribution was retained, but no spatial structure was visible. For the homogeneous case the mean values given in Table 1 were applied.

In order to quantify the effects of the spatial structure and variability of soil hydraulic properties on runoff generation comparative modelling with the five spatial concepts was carried out. The observed distribution was assumed to be the 'true' underlying spatial structure of soil hydraulic properties. The soil depths, all of the initial and the boundary conditions, the global parameters as well as the finite element mesh were kept constant throughout the comparative model runs. In the following focus is on the fast runoff components (surface + macropore runoff), because a decrease of these runoff components will cause at long-term an increase of the slow runoff component of the same amount (neglecting the effect of soil water content on evapotranspiration). For Fig. 6 the absolute error between the fast runoff simulated by the observed distribution and the fast runoff simulated by the respective spatial concept was calculated for every time step and cumulated. It is clearly visible that for the different spatial concepts large errors occur for the same time steps. The highest sum of absolute errors was found for the homogenous approach, followed by the stochastic simulation. Half of the error sum detected for the homogeneous case was calculated for the random case and the choropleth map. Roughly ⅓ of the error sum of the homogeneous case was detected for the conditional stochastic simulation providing the overall smallest errors. An analogous computation of the root mean square error, which is more sensitive to large errors than a mean absolute error, gives practically the same picture (Table 3). Looking at the reproduction of the overall sum of the fast runoff

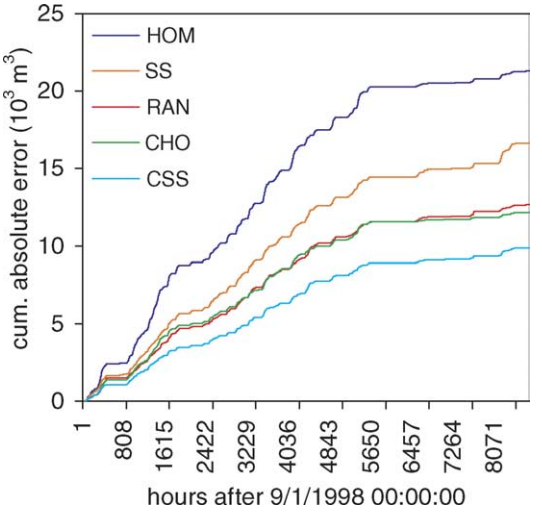

Fig. 6. Cumulative absolute error of the sum of macropore and surface runoff for the homogeneous case (HOM), the random case (RAN), the choropleth map (CHO), the stochastic simulation (SS), and the conditional stochastic simulation (CSS).

components yields a slightly different result. Again the highest deviation was determined for the homogeneous case with an underestimation of the total fast runoff amount by 10%. Significant deviations were also found for the choropleth map with an underestimation of 6%. The conditional stochastic simulation provided an underestimation of 4%, whereas the underestimation of the fast runoff sum caused by the random case and the stochastic simulation was negligible. A quite similar result was detected regarding peak runoff (Fig. 7). In total 13 runoff events were selected, and the difference between peak runoff for the different spatial concepts of the fast runoff components and the respective peak runoff of the observed spatial distribution was calculated. Again the homogeneous case yields the highest deviations, followed by the choropleth map. The stochastic simulation provided moderate deviations, with a clear underestimation of peak runoff for event number 10, which is the event with the highest precipiation rate (20.3 mm h^{-1}) during the simulation period. The conditional stochastic simulation provided on average slightly smaller deviations than the stochastic simulation, whereas the random distribution produced the smallest deviations. Furthermore, Fig. 7 clearly shows that the spatial concepts behave differently for the different runoff events.

Table 3 also shows that all errors introduced by the different spatial concepts are negligible for the actual evapotranspiration. This holds for the temporal course of the actual evapotranspiration, proved by the RMSE, as well as for the total sum of the simulation period.

Table 3
Root mean square error (RMSE) for the single timesteps and relative deviation Δ_{sum} of the total sum of macropore and surface runoff as well as actual evapotranspiration related to the observed distribution

Spatial concept	Actual evapotranspiration		Macropore + surface runoff	
	RMSE (mm h^{-1})	Δ_{sum}	RMSE (mm h^{-1})	Δ_{sum}
Choropleth map	0.0005	0.009	0.71	−0.056
Homogeneous	0.0014	0.024	1.30	−0.102
Random	0.0018	0.029	0.73	−0.002
Stochastic simulation	0.0016	0.027	0.96	−0.009
Conditional stochastic simulation	0.0012	0.014	0.45	−0.039

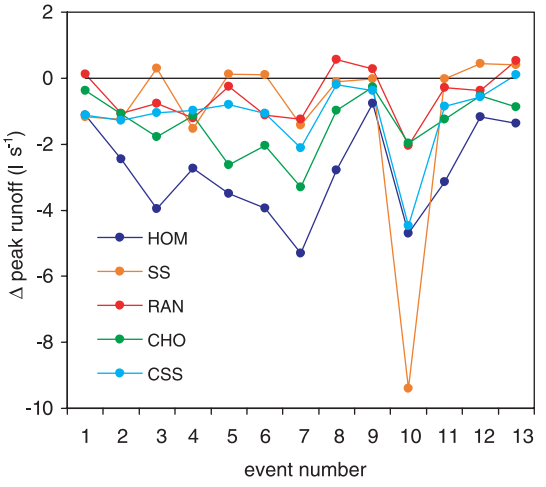

Fig. 7. Difference in peak flow of the fast runoff components for the homogeneous case (HOM), the random case (RAN), the choropleth map (CHO), the stochastic simulation (SS), and the conditional stochastic simulation (CSS). The time steps for the event numbers 1–13 are 139, 152, 371, 1069, 1496, 1695, 3564, 4144, 4223, 4381, 4914, 5252, 5448, respectively.

4. Discussion

After calibration the process model yields a reasonable agreement to the measured hydrograph. The simplified approach for the macropore runoff, neglecting interaction with the soil matrix, was supposed to show difficulties for small rainfall events, because the water entering the macropore system might probably infiltrate across the macropore boundary into the soil matrix without generating any runoff. But obviously these small events are rather sparse as the hydrograph is basically well described by the model. Also the simple runoff delay module and the way the groundwater runoff is treated by the model provided an appropriate process description.

A significant sensitivity was detected for the modelling of runoff generation towards the spatial variation of soil hydraulic parameters, which basically contributes to the findings of other authors (Binley et al., 1989b; Grayson et al., 1995; Merz and Bardossy, 1998). Any spatial aggregation bears a significant decrease of the fast runoff sum and peak runoff. The use of a single spatial mean for the whole catchment (*homogeneous* case) yields a 10% decrease in fast runoff. Roughly half of this value, but still a significant decrease, was found for the modelling based on spatial average values for the conventional soil map (choropleth approach). This demonstrates that a spatial averaging is rather inappropriate due to the non-linearity of the runoff process. The most sensible parameter is probably topsoil K_s (Binley et al., 1989b; Loague, 1988; Loague and Corwin, 1996). For the infiltration process, the averaging causes a loss of locations with small hydraulic saturated conductivities, which are the ones producing the highest amount of infiltration excess. A modelling based on a spatial pattern, which has the same frequency distribution as the observed distribution, thus should yield the same fast runoff amount as the observed distribution, if a downslope re-infiltration process is not considered. This was found for the random case and the stochastic simulation, which provide both an almost exact reproduction to the overall sum of surface and macropore runoff. With the stochastic simulation a slightly smaller overall sum of fast runoff was calculated than for the random case. This probably results from an approximated frequency distribution of the observed data for the stochastic simulation, whereas the frequency distribution was identical for the random case. Only the coordinates were randomly distributed. For the conditional stochastic simulation a little larger deviation of the fast runoff sum was detected, which might be the result of a slightly worse reproduction of the observed frequency distribution due to the conditioning of the stochastic simulation. Due to the smoothing effect of the kriging, also detected by Loague and Kyriadikis (1997), the frequency distribution exhibits a slight bias. However, the deviation introduced by the conditional stochastic simulation is only half the error introduced by the averaging for the choropleth map.

Compared to the overall sum of fast runoff for the one year, the temporal course of runoff is more relevant, if an adequate process description is requested. The reproduction of the temporal course of fast runoff with the five spatial concepts was of different quality. The approaches that preserved the observed spatial organisation (choropleth map and conditional stochastic simulation) exhibited the smallest root mean square errors. But the conditional stochastic simulation produced roughly only half the error of the choropleth map, although for this approach the number of polygons was supposed to be large enough to preserve the topology. The random case showed an RMSE only slightly higher than the choropleth map, which might be a hint to the fact that even for the temporal course of fast runoff the frequency distribution plays an important role. The stochastic simulation showed an even higher RMSE, although this result is a bit difficult to interpret, because only a single realization was considered for this study. Fig. 5 reveals that even the stochastic approach shows a certain topology, which in this case does not resemble the observed distribution topology. The use of an ensemble average of e.g. 50 realizations will probably lead to a RMSE comparable to the one of the random approach. Merz and Bardossy (1998) detected that structured variability yielded much larger runoff amounts than a stochastic variability. This strong effect was not observed during this study, although for our study also the structured spatial concepts exhibited the best reproduction of the observed

distributions' hydrograph. The strengths of this effect clearly depends on the consideration of a re-infiltration process. For the model of Merz and Bardossy (1998) re-infiltration was considered, thus the infiltration excess generated somewhere at an upslope low conductivity location in the catchment could re-infiltrate at a downslope high conductivity location for a random spatial distribution. In our study any infiltration excess was routed to the channel without the opportunity to re-infiltrate. However, the relevance of this process probably depends on site-specific characteristics like topography, land use and also on the model scale. In this study not a sheet flow over the soil surface was assumed, but a linear concentration of runoff (Moore et al., 1988) within a grid cell of 10 m^2. However, the relevance of re-infiltration is still debated (Loague and Kyriadikis, 1997). Due to the process model structure applied in this study, the spatial correlation between flow length to the channel and topsoil K_s dominates the fast runoff processes. The coefficient of correlation between flow length and topsoil K_s of the observed distribution is 0.67. Fig. 8 shows that with increasing flow length the K_s-values also increase, which is basically resembled by the conditional stochastic simulation. For this spatial distribution the coefficient of correlation between flow length and topsoil K_s is 0.65, whereas the spatial correlation between topsoil K_s and flow length is negligible for the random case and the non-conditional stochastic simulation ($r=0.02$ and $r=0.09$, respectively). The reason for the best agreement between process model results of the conditional stochastic simulation and the observed spatial distribution is probably the fact that this correlation between topsoil K_s and flow length to the channel is preserved.

In the introduction the question was raised which spatial concept is the most appropriate. The discussion on that topic should probably be carried out against the background of the required information level. The conditional stochastic simulation seems to be the most appropriate, because it showed clearly the smallest RMSE of the five spatial concepts, indicating the best reproduction of the fast runoff. Further the deviation of the total sum of fast runoff was even smaller than for the choropleth map, which is probably the second best approach. For the conditional stochastic

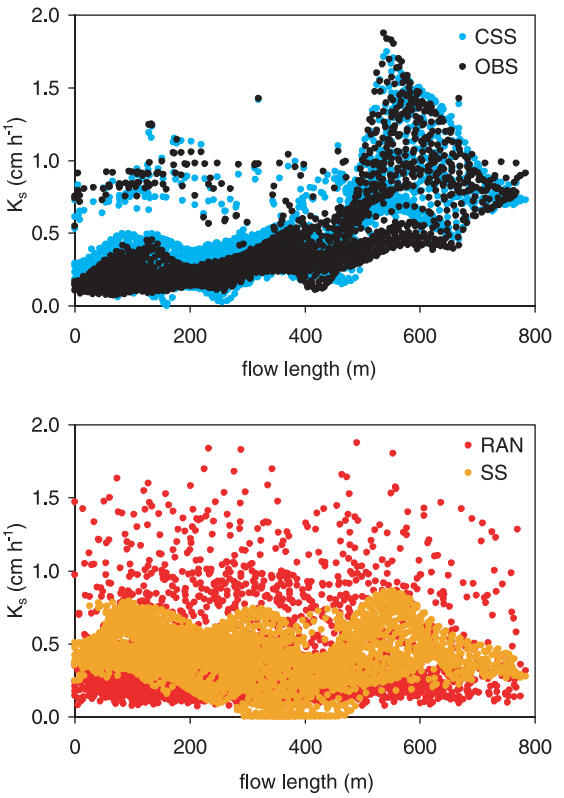

Fig. 8. Scatter plot between the flow length to the channel and topsoil K_s of the observed spatial distribution (OBS), the conditional stochastic simulation (CSS), the random case (RAN) and the stochastic simulation (SS).

simulation the spatial co-variance function and a minimum number of sample point values is required, but even for the choropleth map a certain number of sample points is required, otherwise the averaging for single polygons becomes erroneous. How well one of these two spatial concepts will behave in the end of course depends on the sample point number or the number of polygons, respectively. Among these two approaches, the conditional stochastic simulation has the advantage that, besides resembling the spatial topology, the frequency distribution is better preserved than for the choropleth map. Seyfried and Wilcox (1995) distinguish between a stochastic and a deterministic (organised) spatial variability. Conditional stochastic simulations are seen as an appropriate method to incorporate both, the stochastic and the deterministic component, for the description of catchment scale soil spatial variation.

5. Summary and conclusions

A three-dimensional hydrological model was established accounting for canopy interception, evapotranspiration, surface and macropore runoff as well as for groundwater runoff. This continuous model was applied to the 28.6 ha 'Berrensiefen' catchment for a simulation period of one year. The process model was validated for total runoff, based on an observed distribution of soil hydraulic properties, which were assumed to be layered in vertical and continuous in horizontal direction. Comparative modelling with five spatial distributions of soil hydraulic parameters revealed a sensitivity of runoff generation towards the spatial variation of soil hydraulic properties. For the catchment used in this study and under the given atmospheric boundary conditions the detected sensitivity was significant, but still rather moderate. In general the sensitivity of runoff to the spatial variation of soil hydraulic properties depends on the variability of soil parameters, in particular of the topsoil K_s, in relation to the frequency distribution of the precipitation. For a continuous modelling a high sensitivity will probably be given if the mean of K_s and the mean of precipitation events are rather close to each other. A spatial aggregation of soil hydraulic parameters bears a loss of fast runoff components, indicating that the preservation of the frequency distribution is of large importance. Against the background of the overall fast runoff sum, it is concluded that any approach including an aggregation, such as a choropleth map, is rather inappropriate. But not only is the total amount of fast runoff of relevance. For runoff concentration in time the spatial topology of soil hydraulic parameters is relevant, too. The runoff has to be predicted at the correct amount, but also at the correct location. Otherwise the hydrograph will not be reproducible. Furthermore, it is concluded that the spatial topology should be preserved, indicating that a purely stochastic variability, e.g. generated with a stochastic simulation is rather insufficient. This task is even better performed with a choropleth map, although this approach bears the difficulties mentioned above. A conditional stochastic simulation is seen as the most suitable approach, because it preserves the frequency distribution as well as the topology (deterministic variability), although both features were only approximated. The relevance of deterministic spatial structure for runoff generation depends on the scale dependent process of re-infiltration. We recommend the use of conditional stochastic simulations for soil hydraulic properties in the context of distributed hydrological modelling, because this approach presented the best compromise for preserving the frequency distribution and the spatial topology of the sampled data.

Acknowledgements

This work was supported by the German Research Foundation (post graduate school 437: Relief-a structured and variable boundary layer).

References

Abbott, M.B., Bathurst, J.C., O'Connel, P.E., Rasmussen, J., 1986. An introduction to the European Hydrological System—Systeme Hydrologique Europeen, 'SHE', 2. Structure of a physically-based, distributed modelling system. Journal of Hydrology 87, 61–77.

Armstrong, M., 1998. Basic Linear Geostatistics. Springer, New York. 149 pp.

Beven, K., 2001. How far can we go in distributed hydrological modelling? Hydrology and Earth System Sciences 5 (1), 1–12.

Beven, K.J., Calver, A., Morris, E.M., 1987. The Institute of Hydrology distributed model. UK Institute of Hydrology. Report No. 98, Wallingford, Oxon, United Kingdom.

Binley, A., Beven, K., 1992. Three-dimensional modelling of hillslope hydrology. In: Beven, K.J., Moore, I.D. (Eds.), Terrain Analysis and Distributed Modelling in Hyrology. Advances in Hydrological Processes. Wiley, Chichester, pp. 107–119.

Binley, A., Elgy, J., Beven, K., 1989a. A physically based model of heterogeneous hillslopes. 1. Runoff production. Water Resources Research 25 (6), 1219–1226.

Binley, A., Beven, K., Elgy, J., 1989b. A physically based model of heterogeneous hillslopes 2. Effective hydraulic conductivities. Water Resources Research 25 (6), 1227–1233.

Bogena, H., Diekkrüger, B., Klingel, K., Jantos, K., Thein, J., 2003. Analysing and modelling solute and sediment transport in the catchment of the Wahnbach river. Physics and Chemistry of the Earth 28, 227–237.

Brakensiek, D.L., Rawls, W.J., 1994. Soil containing rock fragments: effects on infiltration. Catena 23, 99–110.

Bronstert, A., Bárdossy, A., 1999. The role of spatial variability of soil moisture for modelling surface runoff generation at the small catchment scale. Hydrology and Earth System Sciences 3 (4), 506–516.

Bronstert, A., Plate, E.J., 1997. Modelling of runoff generation and soil moisture dynamics for hillslopes and micro-catchments. Journal of Hydrology 198, 177–195.

Burrough, P.A., 1993. Soil variability: a late 20th century view. Soils and Fertilizers 56 (5), 529–562.

Deutsch, C.V., Journel, A.G., 1998. GSLIB: Geostatistical Software Library and User's Guide, Applied Geostatistics Series, second ed. Oxford University Press, Oxford, 369 pp.

FAO, ISRIC, ISSS, 1998. World Reference Base for Soil Resources. World Soil Resources Report No. 84. FAO, Rome, Italy.

Feddes, R.A., Kowalik, P.J., Zaradny, H., 1978. Simulation of field water use and crop yield. Simulation Monographs, Wageningen, 188 pp.

Freeman, T.G., 1991. Calculating catchment area with divergent flow based on a regular grid. Computers and Geoscience 17 (5), 709–717.

Freeze, R.A., 1971. Three-dimensional, transient, saturated-unsaturated flow in a groundwater basin. Water Resources Research 7 (2), 347–366.

Grayson, R., Blöschl, G. (Eds.), 2001. Spatial Patterns in Catchment Hydrology; Observations and Modelling. University Press, Cambridge, p. 404.

Grayson, R.B., Blöschl, G., Moore, I.D., 1995. Distributed parameter hydrologic modelling using vector elevation data: THALES and TAPES-C. In: Singh, V.P. (Ed.), Computer Models of Watershed Hydrology. Water Resources Publications, Highlands Ranch, Colorado, pp. 669–696 (Chapter 19).

Herbst, M., Diekkrüger, B., 2003. Modelling the spatial variability of soil moisture in a micro-scale catchment and comparison with field data using geostatistics. Physics and Chemistry of the Earth 28, 239–245.

Herbst, M., Diekkrüger, B., Vereecken, H., 2006. Geostatistical co-regionalization of soil hydraulic properties in a micro-scale catchment using terrain attributes. Geoderma in press.

Heuvelink, G.B.M., Webster, R., 2001. Modelling soil variation: past, present, and future. Geoderma 100, 269–301.

Hodgkinson, R.A., Armstrong, A.C., 1996. Field studies of runoff processes on restored land in South Wales and the design of channels for erosion control. In: Anderson, M.G., Brooks, S.M. (Eds.), Advances in Hillslope Processes. Wiley, Chichester, pp. 613–633.

Loague, K.M., 1988. Impact of rainfall and soil hydraulic property information on runoff predictions at the hillslope scale. Water Resources Research 24 (9), 1501–1510.

Loague, K., Corwin, D.L., 1996. Uncertainty in regional-scale assessments of non-point source pollutants. In: Corwin, D.L., Loague, K., (Eds.), Applications of GIS to the Modeling of Non-point Source Pollutants in the Vadose Zone. SSSA Special Publication 48, pp. 131–152.

Loague, K., Kyriakidis, P.C., 1997. Spatial and temporal variability in the R-5 infiltration data set: Déjà vu and rainfall-runoff simulations. Water Resources Research 33 (12), 2883–2895.

Loague, K., VanderKwaak, J.E., 2004. Physics-based hydrologic response simulation: platinum bridge, 1958 Edsel, or useful tool. Hydrological Processes 18, 2949–2956.

Loague, K., Heppner, C.S., Abrams, R.H., Carr, A.E., VanderKwaak, J.E., Ebel, B.A., 2005. Further testing of the Integrated Hydrology Model (InHM): event-based simulations for a small rangeland catchment located near Chickasha, Oklahoma. Hydrological Processes 19, 1373–1398.

Mantoglou, A., Wilson, J.L., 1982. The turning bands method for simulation of random fields using line generation by a spectral method. Water Resources Research 18, 1379–1394.

Matheron, G., 1973. The intrinsic random functions and their applications. Advances in Applied Probability 5, 439–468.

Merz, B., Bárdossy, A., 1998. Effects of spatial variability on the rainfall runoff process in a small loess catchment. Journal of Hydrology 212–213, 304–317.

Merz, B., Plate, E.J., 1997. An analysis of the effects of spatial variability of soil and soil moisture on runoff. Water Resources Research 33 (12), 2909–2922.

Minasny, B., McBratney, A.B., Whelan, B.M., 1999. Vesper Version 1.0. www.usyd.edu.au/su/agric/acpa.

Monteith, J.L., 1975. Vegetation and the Atmosphere. Academic Press, New York. 439 pp.

Moore, I.D., Burch, G.J., Mackenzie, D.H., 1988. Topographic effects on the distribution of surface soil water and the location of ephemeral gullies. American Society of Agricultural Engineers 31 (4), 1098–1107.

Nash, J.E., Sutcliffe, J.V., 1970. River flow forecasting through conceptual models: part I —A discussion of principles. Journal of Hydrology 10, 282–290.

Odeh, I.O.A., McBratney, A.B., Chittleborough, D.J., 1995. Further results on prediction of soil properties from terrain attributes: heterotropic cokriging and regression-kriging. Geoderma 67, 215–226.

Paniconi, C., Wood, E.F., 1993. A detailed model for simulation of catchment scale subsurface hydrologic processes. Water Resources Research 29 (6), 1601–1620.

Rawls, W.J., Brakensiek, D.L., 1985. Prediction of soil water properties for hydrologic modelling. American Society of Civil Engineers, 293–299.

Rutter, A.J., Morton, A.J., Robins, P.C., 1975. A predictive model of rainfall interception in forests 2. Generalization of the model and comparison with observations in some coniferous and hardwood stands. Journal of Applied Ecology 12, 367–380.

Seyfried, M.S., Wilcox, B.P., 1995. Scale and the nature of spatial variability: field examples having implications for hydrologic modeling. Water Resources Research 31 (1), 173–184.

Šimůnek, J., Huang, K., van Genuchten, M.T., 1995. The SWMS_3d Code for Simulating Water Flow and Solute Transport in Three-dimensional Variably-saturated Media, Version 1.0. Research Report No. 139. United States Salinity Laboratory Riverside. California. 155 pp.

van Genuchten, M.Th., 1980. A closed form eqation for predicting the hydraulic conductivity of unsaturated soils. Soil Science Society of America Journal 44, 892–898.

VanderKwaak, J.E., Loague, K., 2001. Hydrologic-response simulations for the R-5 catchment with a comprehensive physics-based model. Water Resources Research 37, 999–1013.

Vereecken, H., Herbst, M., 2005. Statistical regression. In: Pachepsky, Y., Rawls, W.J., (Eds.), Development of Pedotransfer Functions in Soil Hydrology. Developments in Soil Science, vol. 30, pp. 3–19.

Vereecken, H., Kaiser, R., Dust, M., Pütz, T., 1997. Evaluation of the multistep outflow method for the determination of unsaturated hydraulic properties of soils. Soil Science 162 (9), 618–631.

Wackernagel, H., 1995. Multivariate Geostatistics: An Introduction with Applications, second ed. Springer, New York (completely revised) 291 pp.

Warrick, A.W., Nielsen, D.R., 1980. Spatial variability of soil physical properties in the field. In: Hillel, D. (Ed.), Application of Soil Physics. Academic Press, New York, pp. 319–344.

Webster, R., 2000. Is soil variation random? Geoderma 97, 149–163.

Willmott, C.J., 1981. On the validation of models. Physical Geography 2.

Zehe, E., Blöschl, G., 2004. Predictability of hydrologic response at the plot and catchment scales: role of initial conditions. Water Resources Research 40, W10202. doi:10.1029/2003WR002869.

Zhu, A.X., Mackay, D.S., 2001. Effects of spatial detail of soil information on watershed modeling. Journal of Hydrology 248, 54–77.